Proceedings of DETC '04:
ASME 2004 International Design Engineering Technical Conferences
And Computers and Information in Engineering Conference
September 28 - October 2, 2004, Salt Lake City, Utah

DRAFT - DETC04/DFM - 0000

ESTIMATION OF PRODUCT RESPONSE: THE EMPIRICAL SIMILITUDE METHOD AND TECHNIQUE OF CONFORMAL MAPPING

Srikanth Tadepalli
Department of Mechanical Engineering
The University of Texas at Austin
Austin, TX 78712
tsrikanth@mail.utexas.edu

Dr. Kristin L. Wood
Department of Mechanical Engineering
The University of Texas at Austin
Austin, TX 78712
wood@mail.utexas.edu

Dr. Richard H. Crawford
Department of Mechanical Engineering
The University of Texas at Austin
Austin, TX 78712
rhc@mail.utexas.edu

Dr. Patricio F. Mendez
Department of Materials Science and Engineering
Massachusetts Institute of Technology
Cambridge, MA 02139
pat@mit.edu

Brian L. Doud
Department of Mechanical Engineering
The University of Texas at Austin
Austin, TX 78712
bdoud@hotmail.com

ABSTRACT

Functional testing of representative prototypes is an important phase in the evolution of most products. Layer Fabrication methods, importantly the Selective Laser Sintering (SLS) process allow for quick fabrication of test prototypes such that the experimental data derived from them can be used to predict the response of a hypothetical product for a desired variable of interest.

Traditional Similitude Method (TSM) or Buckingham π theorem has been used conventionally for dimensional analysis to correlate the similarity between different structures. Some of its inherent limitations have prompted researchers to include the effects of non-linear material variations and geometric distortions during the scaling process. Thus, the development of the Empirical Similitude Method (ESM) is largely based on the hypothesis that these non-linear variations and distortions can be captured mathematically by using intermediate test specimens. In an effort to improve ESM, conformal mapping has been hypothesized to be an important technique for scaling and analysis. This paper explores the technique of Conformal Mapping as a potential equivalence procedure based on the principle of ESM. The methodology is elucidated along with a stress and a heat transfer example.

1.0 INTRODUCTION

Similitude and prediction analysis gains significance when a design is to be evaluated for different performance criteria. The idea of TSM evaluation is based on the assertion that an entity defining a parameter of a given system can be roughly estimated by the value of the same parameter in another system, as long as the two systems share a common similarity, using the fundamental dimensions of mass [M], length [L], time [T], temperature [θ] and solid angle [α] (ignoring the fundamental dimension in the domain of optics). This is possible because the variables of interest and the system parameters are dimensionally same irrespective of the numerical value that they can achieve, and have to be consistent according to Fourier's Law of dimensional homogeneity. The term physical similarity here defines the range of applicability of TSM and can be best described as the governing equation of the variable of interest in terms of the system parameters. Hence, to make an accurate prediction, the two systems in question must have physical similarity along with geometric and parametric similarity [Szirtes, 1998; Bridgman, 1931].

This paper explains TSM, and then elaborates on ESM, a method that builds on the existing methodology of TSM by incorporating non-linear material variations and geometric distortions. The technique of conformal mapping is then elucidated to predict product behavior based on the empirical data gathered in the testing of its characteristic rapid prototyping (RP) model. RP models are used for evaluation as they offer the flexibility of repeated evaluation for any given complex geometry.

2.0 BACKGROUND

tech

Suppose two similar systems, called model and product systems for convenience, are respectively defined as:

$$f(x_{m,1}, x_{m,2}, \ldots\ldots\ldots\ldots\ldots\ldots\ldots, x_{m,n}) = 0 \qquad (1)$$

$$f(x_{p,1}, x_{p,2}, \ldots\ldots\ldots\ldots\ldots\ldots\ldots, x_{p,n}) = 0 \qquad (2)$$

where $x_{m/p,i}$ are the same system variables for the model and the product that govern the behavior of each, $\forall\ i \in [1,n]$. If the variable of interest is y (which is a desired output or one of state variables), the two equations can be expressed in terms of y as:

$$y_m = g\,(x_{m,1}, x_{m,2}, \ldots\ldots\ldots\ldots\ldots\ldots, x_{m,n-1}) \quad (3)$$
$$y_p = g\,(x_{p,1}, x_{p,2}, \ldots\ldots\ldots\ldots\ldots\ldots, x_{p,n-1}) \quad (4)$$

The number of factors or parameters is reduced by 1, as there is loss of one degree of freedom due to the state representation in terms of the variable of interest. According to Buckingham's π theorem, the states can be modeled in terms of dimensionless π parameters as:

$$f^*(\pi_{m,1}, \pi_{m,2}, \ldots\ldots\ldots\ldots\ldots\ldots, \pi_{m,N}) = 0 \quad (5)$$
$$f^*(\pi_{p,1}, \pi_{p,2}, \ldots\ldots\ldots\ldots\ldots\ldots, \pi_{p,N}) = 0 \quad (6)$$
$$\pi_{m,y} = g^*(\pi_{m,1}, \pi_{m,2}, \ldots\ldots\ldots\ldots\ldots\ldots, \pi_{m,N-1}) \quad (7)$$
$$\pi_{p,y} = g^*(\pi_{p,1}, \pi_{p,2}, \ldots\ldots\ldots\ldots\ldots\ldots, \pi_{p,N-1}) \quad (8)$$

Hence, for these two corresponding systems, the Buckingham π theorem can be generalized as [Dutson, 2002]

$$\pi_{p,y}\,(P_p) = \pi_{m,y}\,(P_m) \quad (9)$$

if

$$\pi_{m,i} = \pi_{p,i}\ \forall\ i \in [1, N-1] \quad (10)$$

where P is the parameter of interest. Equation (9) is called the *prediction equation* while Equation (10) signifies the *similarity constraints*. The combination is generally referred to as the *model laws*. The number of dimensionless parameters is now N such that $N = n - r$ and hence far smaller in number ($N < n$) and easier to manipulate. The variables n and r respectively represent the original number of system parameters and the number of independent parameters in the given system parameter set. Mathematically, r represents the rank (the number of independent rows or columns in a matrix) of the dimensional matrix formed using the system parameters.

The influence of TSM on prediction analysis in the process of design and manufacture is best illustrated with a standard example of a fluid mechanics problem [Dutson, 2002]. If the drag force experienced by a submarine or any submerged body is the variable of interest, the sheer size and magnitude and the time and expenditure involved in full-scale prototype testing makes the TSM a viable option. Proceeding with the analysis,

$$D = f\,(l, V, \rho, \mu) \quad (11)$$

where D is drag force, l is the characteristic length, V is the velocity of the submarine, ρ is the fluid density and μ is the dynamic viscosity of the fluid. Setting up the dimensional matrix, we have,

Table 1. Dimensional Matrix

	l	V	ρ	D	μ
M	0	0	1	1	1
L	1	1	-3	1	-1
T	0	-2	0	-2	-1

Since D is the variable of interest, selecting l, V and ρ as the *repeating variables* (variables that replace the fundamental dimensions), we have,

Table 2. Echelon Matrix

	l	V	ρ	D	μ
l [L]	1	0	0	2	1
V [LT^{-1}]	0	1	0	2	1
ρ [ML^{-3}]	0	0	1	1	1

The matrix thus formed, referred to as the *Echelon Matrix* is actually a matrix transformation such that the repeating variables combine to from a diagonal matrix where the element along the diagonal is 1. This transformation causes a change in the exponent or power of the dependent variables to provide for the dimensionless π parameters. In this example, we have,

$$\pi_1 = \frac{D}{l^2 V^2 \rho} \quad ; \quad \pi_2 = \frac{\mu}{lV\rho} \quad (12)$$

As can be seen from the denominators of the two fractions, the π parameters can be expressed as functions of one another. Hence,

$$\pi_1 = f(\pi_2) \quad or \quad \frac{D}{\rho V^2 l^2} = f\left(\frac{\mu}{\rho V l}\right) \quad (13)$$

and therefore for two physically similar systems, we have,

$$\left(\frac{D}{\rho V^2 l^2}\right)_p = \left(\frac{D}{\rho V^2 l^2}\right)_m if \left(\frac{\mu}{\rho V l}\right)_p = \left(\frac{\mu}{\rho V l}\right)_m \quad (14)$$

The two factors defined above are of utmost importance as they physically characterize and identify the drag coefficient (C_D) and the Reynolds's Number (R_e) thereby describing the type of fluid flow. Hence,

$$C_{D,p} = C_{D,m} \ \ if \ \ R_p = R_m \quad (15)$$

By observation and calculation we could conclude that unless the two systems are scaled in the same environment, TSM would fail. This implies, that if the model is scaled in such a way that the R_e is indicative of laminar flow, then it cannot be used to predict the behavior of the submarine in turbulent regime, as would be the case if R_e is also scaled to the same degree or magnitude.

This procedure not only serves to show the versatility of TSM but also shows the limitations and drawbacks in using the procedure unless proper care is taken during analysis. One of the major assumptions that is been made during the analysis is that the variables of interest would map *one-to-one* or *linearly*, which is not always true. Another significant assumption made is that there is no distortion (geometric discontinuities) in the models or in the geometries or in the material behavior of the systems under consideration for different environmental conditions. In other words, the material is pre-supposed to be isotropic and the boundary conditions to be constant and uniform throughout the entire range of study.

These factors illustrate the limitations of TSM and therefore impose the need for an analysis tool that takes into consideration all of the working properties and constraints in a dynamic environment. Hence the development of an innovative similitude procedure called *Empirical Similitude Method* that extends the correlation between the model and the product empirically, rather than with dimensional information alone [Cho, 1999].

The Empirical Similitude Method comes into play under the following conditions:

- The two systems have parameters in their governing equations that have a non-linear behavior for a given condition.
- The material properties of the systems vary from point to point.
- The conditions are not uniform and constant throughout the entire range of application.
- The system under consideration is comprised of multiple materials and hence various responses and varying behaviors.
- The specimens in the study have distortions in their geometries or parameters.

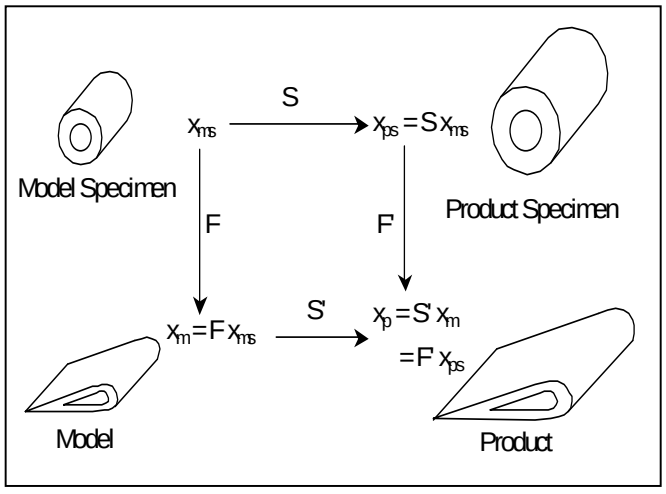

Figure 1. Empirical Similarity Method, Adapted from [Cho, 1999]

The concept of ESM establishes a correlation between the model and the product through empirical testing as illustrated in Figure 1 [Dutson, 2002]. Instead of using a direct mapping between the model and the product (which is not always accurate due to the above mentioned reasons), the procedure employs the use of intermediate specimens (as test specimens) called the model and the product specimen, which are indicative of the model and the product respectively. The model specimen, which is a geometrically simplified version of the model, is made from the same material and the manufacturing process as the model and the product specimen, which is a geometrically simplified version of the product, is made from the same material and the manufacturing process as the product.

If the state vectors (written in bold) of the model specimen, the model, the product specimen and the product are respectively $\boldsymbol{x}_{ms}$, $\boldsymbol{x}_m$, $\boldsymbol{x}_{ps}$, and $\boldsymbol{x}_p$, then,

$$\boldsymbol{x}_p = \boldsymbol{f}(\boldsymbol{x}_{ms}, \boldsymbol{x}_m, \boldsymbol{x}_{ps}) \tag{16}$$

The relationship between any two vectors can be given by a fully populated transformation matrix, the use of which forms the basis of ESM. The test data of the model and the model specimen is used to define a *scale transformation matrix S* that maps the information in the shape or geometric domain and the test data of the model specimen and the product specimen is used to generate a *form transformation matrix F* that maps the material information [Dutson, 2002]. Hence the product of these two matrices along with the model (model specimen) state vector should in principle give the response of the product. Mathematically, the response can be shown as:

$$\boldsymbol{x}_{ps} = \boldsymbol{S}\,\boldsymbol{x}_{ms} \tag{17}$$
$$\boldsymbol{x}_m = \boldsymbol{F}\,\boldsymbol{x}_{ms} \tag{18}$$
$$\boldsymbol{x}_p = (\boldsymbol{S} \times \boldsymbol{F})\,\boldsymbol{x}_{ms} \tag{19}$$

As can be seen from Figure 1, there are two distinct paths to arrive at the product state vector and hence,

$$\boldsymbol{x}_p = (\boldsymbol{S'} \times \boldsymbol{F'})\,\boldsymbol{x}_{ms} \tag{20}$$

This is possible since the ESM assumes the shape and the form transformation matrices to be independent of each other. Further, the model and the product specimens are representative of the model and the product respectively. Hence the product of the scale and form transformation matrices is assumed to be equal throughout and unique to a given system. Therefore,

$$\boldsymbol{S} \times \boldsymbol{F} = \boldsymbol{S'} \times \boldsymbol{F'} \text{ and } \boldsymbol{S} = \boldsymbol{S'},\ \boldsymbol{F} = \boldsymbol{F'} \tag{21}$$

Another important observation is that the necessity to identify and quantify the variables that affect the system is minimized as the numerical value of the test results conveys the required information rather than the values of the

influencing parameters. Elaborating, if the product assumed to be a cantilever beam, is to be evaluated for deflection, then the deflection values of the model and the specimens can be coupled to obtain an estimate for the product. The procedure therefore minimizes the necessity to identify all system variables (in this case the load, Young's modulus, moment of inertia and geometry) and scale each one of them.

3.0 CONFORMAL MAPPING -- MOTIVATION

Empirical Similitude Method is a novel extension to the process of dimensional analysis as it includes the experimental domain in the analysis procedure. The main aspect of analyzing a system using ESM is to establish and manipulate the transformation matrices such that the prediction mapping over the geometry and material concurs well with the actual values. While the technique has been developed to an extent where most structural and thermal problems can be addressed, a generic methodology is needed to generalize the applicability of the process to a wide range of problems. The objective in advancing ESM is to pursue other analogous scaling procedures, integrate them with ESM and prove the feasibility of the combination.

As part of this effort, conformal mapping , defined as the mapping of a point from one domain to another, is an important technique in mapping parameters from a field where computation is difficult to another sphere where the analysis is much simpler. The essence of the problem and the parameter to be analyzed together with the boundary conditions are to be mapped such that the estimation of the parameter of interest in the new domain corresponds to the actual system parameter. As the model and the product specimens are simplified geometries of the model and the product respectively, a clear perspective is required that assists in mapping a point in a given geometry and the associated response variable in the specimen domain to that in the actual model and product domains.

If the model specimen and the product specimen are experimentally tested for response values, we have,

$$\left[x_{ps}\right] = \left[S\right] \times \left[x_{ms}\right] \tag{22}$$

where

$$\left[S\right]_{n\times n} = \begin{bmatrix} x_{11} & x_{12} & \cdots & x_{1n} \\ x_{21} & x_{22} & \cdots & x_{2n} \\ . & . & & . \\ . & . & & . \\ . & . & & . \\ x_{n1} & x_{n2} & \cdots & x_{nn} \end{bmatrix} \tag{23}$$

The matrix satisfies the Cayley-Hamilton theorem, which states that any square matrix [*B*] has to satisfy its characteristic equation given by

$$\left|\lambda I - B\right| = 0 \tag{24}$$

where *I* is the identity matrix. The determinant allows calculation of the eigenvalues and hence the eigenvectors. The matrix formed by the eigenvalues is diagonal irrespective of the nature (real, complex or complex conjugate) of the eigenvalues as long as they are linearly independent. This implies that for any value attained by a given eigenvalue, there always exists a matrix that is diagonal as long as the condition of linear independence is satisfied. Other elements are changed or altered depending on whether the eigenvalue is real or complex. Consider a simple cantilever deflection problem. The lateral deflection is given by,

$$\delta = \frac{Fl^3}{3EI} \tag{25}$$

or

$$F = \left(\frac{3EI}{l^3}\right)\delta \tag{26}$$

where *F* is the load, *E* is Young's modulus, *I* is moment of inertia and *l* is length of the specimen. The stiffness of the beam is given by the quantity in the parentheses. Simplifying and generalizing,

$$\vec{F} = [K]\vec{\delta} \tag{27}$$

where [*K*] is the stiffness matrix that accounts for the variations in all directions. The eigenvalues of this matrix gives the stiffness values across different orientations while the eigenvectors represent the deflection along that direction.

If there arises a situation where the eigenvalues are not independent of one another, then another form of interpretation is required which correlates those eigenvalues that are dependent on one another using pairs of complex conjugates. However, the worst case arises when multiple eigenvalues attain complex values. Examining the behavior of the system under the influence of complex eigenvalues requires the assessment of the complex variables that these eigenvalues represent. The mapping of these variables from one domain to another is a possible solution to understand the effects of these complex eigenvalues.

Conformal Mapping is a technique that is used to understand such a correlating phenomenon. This mapping is required since the prediction of the response variables in the product/product specimen depends on both the corresponding response variables in the model/model specimen and the characteristic eigenvalues. If one of these eigenvalues (which indicate the degree of scaling of the response parameters to be performed to map the results) is complex, then according to the definition, at least one of the product response variables is complex.

Any given complex function can be represented in terms of a complex variable, *i.e.,*

$$a + ib = f(x + iy) \tag{28}$$

The variables a, b, x and y are real values. Hence, if the two complex parameters are represented by,

$$z_1 = a + ib \text{ and } z_2 = x + iy \tag{29}$$

then

$$z_1 = f(z_2) \tag{30}$$

The curve traced by z_2 determines the curve that z_1 would trace. This implies that for every value of x and y there exists a unique set of values a and b such that the properties of the function are mapped or transformed from the z_2 field to the z_1 field for single-valued function transformations. Assuming a hypothetical situation where some of the response variables in the product/product specimen matrix are functions of complex variables *i.e.*, the matrix of eigenvalues has complex elements, we have,

$$x_{ps,i} = (a_1 + ib_1)x_{ms,i} \tag{31}$$

$$x_{p,i} = (a_1 + ib_1)x_{m,i} \tag{32}$$

$$x_{m,i} = (a_2 + ib_2)x_{ms,i} \tag{33}$$

$$x_{p,i} = (a_2 + ib_2)x_{ps,i} \tag{34}$$

Equations (31) and (32) capture the system geometries while Equations (33) and (34) capture the system material interactions. If a number of such elements are complex, then the evaluation becomes complicated as the identification and conversion of all the conjugates becomes increasingly difficult especially when the matrices are of higher orders. Hence a possible solution to this is the association of curve tracing with conformal mapping to obtain the scaling laws.

Having described the motivation and necessity behind the research objective, a generalized transformation procedure is described below to illustrate the process.

3.1 THE LOGARITHMIC TRANSFORMATION

One of the simplest transformations among the various possible conversions is the combination of a non - linear transformation and the logarithmic transformation. Most problems that need to be analyzed are simplified using maps but the real task lies in selecting the appropriate transformation that is suitable for the original geometries. Since this map is only in the geometric domain and between two shapes, the material information is not transformed. Intermediate specimens are thus required in the analysis to capture the material interactions. From classical mathematics, a rectangular shape is mapped as a sector of an annulus using the transformation:

$$w_1 = e^{az} \tag{35}$$

(where $w = u + iv$ and $z = x + iy$ are complex functions and u, v, x and y are complex constants) which is the desired form transformation F. The vertical lines of the rectangle are mapped as arcs and the horizontal lines are transformed into rays that form the boundaries of these arcs as shown in Figure 2. If one vertical side of the rectangle (left side say) is aligned to the y-axis, then it maps to a unit circle and the other vertical side would then map to a circle of radius equal to e^{ax}, x measured along the real axis. If one of the horizontal lines (the bottom side say) is aligned to the x-axis, then it would map to another horizontal line in the image space. The top side would then map to a ray, ay in angle, measured from the x-axis.

Further, the model specimen and the product specimen are of similar geometry but are made from different materials. Hence, a non-linear transformation can capture the scaling in material:

$$w_2 = Az^2 + Bz + C \tag{36}$$

The material changes are captured with an analogous scale Transformation S. The quadratic transformation is necessary as the material transformation is pre-supposed to be non-linear between the specimens and the model and the product. Such an assumption is more consistent with the analysis procedure as any material distortions are captured in the quadratic transformation. Further, since the curve is a second degree complex polynomial, another set of intermediate test specimens are required apart from the existing specimen set, the need for which is demonstrated as part the mathematical analysis. However, this not an absolute requirement as is explained later. Modifying the ESM diagram (see Figure 1) illustrated earlier accordingly, we have,

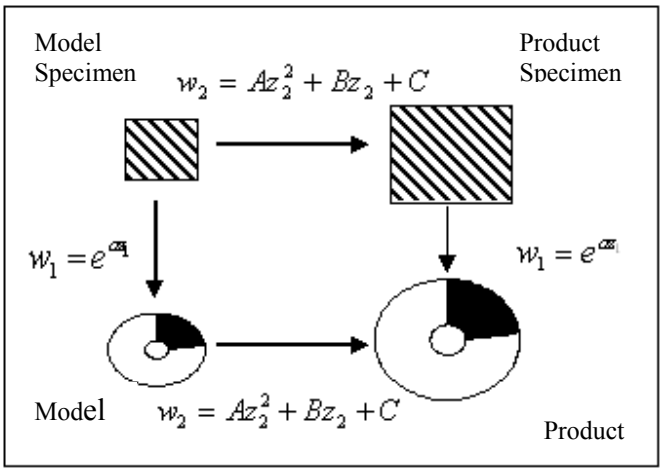

Figure 2. Modified Empirical Similitude Method

Hence the system transformation ($S \times F$) is given by:

$$w = w_1 \times w_2 = \left(Az_2^2 + Bz_2 + C\right)e^{az_1} \tag{37}$$

However, the only portion of the image surface that is really being mapped to is the shaded area shown. Hence, the net scaling factor *a*, is used in the analysis to compensate for the structural distortion.

Formalizing the definition in accordance with conformal mapping,

$$w_m = \exp(az_{ms}) \tag{38}$$

$$w_{ps} = Az_{ms}^2 + Bz_{ms} + C \tag{39}$$

$$z_p = \exp(aw_{ps}) = \exp\{a(Az_{ms}^2 + Bz_{ms} + C)\}$$

$$= \exp\left[a\left\{ \frac{A}{a^2}(\ln w_m)^2 + \frac{B}{a}(\ln w_m) + C \right\} \right] \tag{40}$$

$$u_m + iv_m = \exp\{a(x_{ms} + iy_{ms})\} = \exp(ax_{ms})\exp(iay_{ms})$$

$$= \exp(ax_{ms})(\cos ay_{ms} + i\sin ay_{ms})$$

$$\Rightarrow \frac{u_m}{v_m} = \cot ay_{ms} \Rightarrow a = \frac{1}{y_{ms}}\tan^{-1}\left(\frac{v_m}{u_m}\right) = \frac{\theta_m}{y_{ms}}$$

and

$$\frac{u_m}{v_m} = \cot by'_{ms} \Rightarrow b = \frac{1}{y'_{ms}}\tan^{-1}\left(\frac{v_m}{u_m}\right) = \frac{\theta_m}{y'_{ms}}$$

$$u_{ps} + iv_{ps} = A(x_{ms} + iy_{ms})^2 + B(x_{ms} + iy_{ms}) + C$$

$$\Rightarrow u_{ps} = A(x_{ms}^2 - y_{ms}^2) + Bx_{ms} + C \tag{41}$$

$$v_{ps} = 2Ax_{ms}y_{ms} + By_{ms} \tag{42}$$

Equations (41) and (42) represent the change over the specimen domain However, the two equations have three unknown parameters (*A*, *B* and *C*) and the system of equations is therefore under determined requiring the generation of another equation to have a fully constrained space. Using another set of intermediate test specimens (an intermediate pair of model and product specimen which would generate a set of data points required for analysis), we have,

$$u'_{ps} + iv'_{ps} = A(x'_{ms} + iy'_{ms})^2 + B(x'_{ms} + iy'_{ms}) + C$$

$$\Rightarrow u'_{ps} = A(x'^2_{ms} - y'^2_{ms}) + Bx'_{ms} + C \tag{43}$$

$$v'_{ps} = 2Ax'_{ms}\,y'_{ms} + By'_{ms} \tag{44}$$

The constants remain the same as the scaling has to be consistent between any two sets of specimens. Using the above, the constants *A*, *B* and *C* can be determined. A shortcoming though is that the number of unknown parameters is still three while the number of equations defining these constants is four making the system of equations to be over determined. Since three equations are required to solve for the constants, the equation set can be determined in 4 different ways from Equations (41) through (44). Simplifying, keeping equations (41) and (43) constant and selecting one of Equations (40) and (42) would suffice for solving for the constants. The values obtained can be checked for consistency with either Equation (42) or (40) thereafter. Hence,

$$\begin{bmatrix} u_{ps} \\ v_{ps} \\ v'_{ps} \end{bmatrix} = \begin{bmatrix} (x_{ms}^2 - y_{ms}^2) & x_{ms} & 1 \\ 2x_{ms}y_{ms} & y_{ms} & 0 \\ 2x'_{ms}\,y_{ms} & y'_{ms} & 0 \end{bmatrix} \begin{bmatrix} A \\ B \\ C \end{bmatrix} \tag{45}$$

or

$$\begin{bmatrix} u'_{ps} \\ v_{ps} \\ v'_{ps} \end{bmatrix} = \begin{bmatrix} (x'^2_{ms} - y'^2_{ms}) & x'_{ms} & 1 \\ 2x_{ms}y_{ms} & y_{ms} & 0 \\ 2x'_{ms}\,y_{ms} & y'_{ms} & 0 \end{bmatrix} \begin{bmatrix} A \\ B \\ C \end{bmatrix} \tag{46}$$

such that

$$\begin{bmatrix} u'_{ps} \end{bmatrix} = \begin{bmatrix} (x'^2_{ms} - y'^2_{ms}) & x'_{ms} & 1 \end{bmatrix} \begin{bmatrix} A \\ B \\ C \end{bmatrix} \tag{47}$$

$$\begin{bmatrix} u_{ps} \end{bmatrix} = \begin{bmatrix} (x_{ms}^2 - y_{ms}^2) & x_{ms} & 1 \end{bmatrix} \begin{bmatrix} A \\ B \\ C \end{bmatrix} \tag{48}$$

The determinant of the matrices must be non-zero *i.e.*, the matrices must be non-singular:

$$\det(M) \neq 0$$

$$\Rightarrow y_{ms}\left[x_{ms}y'_{ms} - x'_{ms}\,y_{ms}\right] \neq 0$$

and hence

$$y_{ms} \neq 0 \text{ and } \frac{y'_{ms}}{x'_{ms}} \neq \frac{y_{ms}}{x_{ms}} \tag{49}$$

Combining the constants from the quadratic transformation with the other two constants from the exponential transformation, we have,

$$\begin{bmatrix} A \\ B \\ C \end{bmatrix} = \begin{bmatrix} (x_{ms}^2 - y_{ms}^2) & x_{ms} & 1 \\ 2x_{ms}y_{ms} & y_{ms} & 0 \\ 2x'_{ms}\,y_{ms} & y'_{ms} & 0 \end{bmatrix}^{-1} \begin{bmatrix} u_{ps} \\ v_{ps} \\ v'_{ps} \end{bmatrix}$$

and

$$\begin{bmatrix} a \\ b \end{bmatrix} = \begin{bmatrix} \frac{1}{x_{ms}} & \frac{1}{y_{ms}} \\ \frac{1}{x'_{ms}} & \frac{1}{y'_{ms}} \end{bmatrix} \begin{bmatrix} 0 \\ \theta_m \end{bmatrix} = \theta_m \begin{bmatrix} \frac{1}{y_{ms}} \\ \frac{1}{y'_{ms}} \end{bmatrix} \tag{50}$$

to be the "*constraint equations*" for the "*model equation*" given by,

$$z_p = \exp\left[a\left\{ \frac{A}{a^2}\left(\ln w_m\right)^2 + \frac{B}{a}\left(\ln w_m\right) + C \right\}\right]$$

As can be seen from the matrix definition in Equation (50), since the cross-ratio in Equation (5) is forced to be non-zero, numerical estimates can be obtained for the constants *a* and *b*, signifying non-singular solutions. Further the first constraint forces the imaginary quantity of the first model specimen to be non-zero so that a 2-D evaluation can be obtained in the complex domain. Also the cross ratios $\left(\frac{y'_{ms}}{x'_{ms}}\right)$ and $\left(\frac{y_{ms}}{x_{ms}}\right)$ are forced to be different. This has to be satisfied as an exponential transformation has to be defined for the geometries, which is only possible when *a* and *b* are non-zero as given in Equation (50).

Having outlined the quadratic prediction, a cubic variation is introduced as this produces a consistent equation set and eliminates the inconsistency of the second order polynomial. The mapping for the material transformation is captured using a cubic curve and hence is given by,

$$w_2 = Az^3 + Bz^2 + Cz + D \tag{51}$$

and the system transformation is therefore,

$$w = \left(Az_2^3 + Bz_2^2 + Cz_2 + D\right)e^{az_1} \tag{52}$$

Formalizing the definition in accordance with conformal mapping as before and analyzing,

$$\begin{bmatrix} A \\ B \\ C \\ D \end{bmatrix} = \begin{bmatrix} x_{ms_1}^3 - 3x_{ms_1}y_{ms_1}^2 & (x_{ms_1}^2 - y_{ms_1}^2) & x_{ms_1} & 1 \\ y_{ms_1}^3 - 3x_{ms_1}^2 y_{ms_1} & -2x_{ms_1}y_{ms_1} & -y_{ms_1} & 0 \\ x_{ms_2}^3 - 3x_{ms_2}y_{ms_2}^2 & (x_{ms_2}^2 - y_{ms_2}^2) & x_{ms_2} & 1 \\ y_{ms_2}^3 - 3x_{ms_2}^2 y_{ms_2} & -2x_{ms_2}y_{ms_2} & -y_{ms_2} & 0 \end{bmatrix}^{-1} \begin{bmatrix} u_{ps_1} \\ v_{ps_1} \\ u_{ps_2} \\ v_{ps_2} \end{bmatrix}$$

and

$$\begin{bmatrix} a \\ b \end{bmatrix} = \begin{bmatrix} \frac{1}{x_{ms_1}} & \frac{1}{y_{ms_1}} \\ \frac{1}{x_{ms_2}} & \frac{1}{y_{ms_2}} \end{bmatrix} \begin{bmatrix} 0 \\ \theta_m \end{bmatrix} = \theta_m \begin{bmatrix} \frac{1}{y_{ms_1}} \\ \frac{1}{y_{ms_2}} \end{bmatrix} \tag{53}$$

are the "*constraint equations*" for the "*model equation*" given by,

$$z_p = \exp\left[a\left\{ \frac{A}{a^3}\left(\ln w_m\right)^3 + \frac{B}{a^2}\left(\ln w_m\right)^2 + \frac{C}{a}\left(\ln w_m\right) + D \right\}\right]$$

The quadratic variation was detailed for different cases of the constants. These are valid for the cubic variation as well with relevant changes. The determinant process is extended to the cubic variation with the numerical evaluation of the matrices. It is evident from the matrix definitions above that for the constants *A*, *B*, *C* and *D* to exist, the inverse of the matrix must exist. Hence,

$$\det(M) \neq 0$$

where

$$M = \begin{bmatrix} x_{ms_1}^3 - 3x_{ms_1}y_{ms_1}^2 & (x_{ms_1}^2 - y_{ms_1}^2) & x_{ms_1} & 1 \\ y_{ms_1}^3 - 3x_{ms_1}^2 y_{ms_1} & -2x_{ms_1}y_{ms_1} & -y_{ms_1} & 0 \\ x_{ms_2}^3 - 3x_{ms_2}y_{ms_2}^2 & (x_{ms_2}^2 - y_{ms_2}^2) & x_{ms_2} & 1 \\ y_{ms_2}^3 - 3x_{ms_2}^2 y_{ms_2} & -2x_{ms_2}y_{ms_2} & -y_{ms_2} & 0 \end{bmatrix}$$

or

$$y_{ms_1}, y_{ms_2} \neq 0$$
$$x_{ms_1} \neq \left| \left(x_{ms_2} \pm j\left|y_{ms_1} \pm y_{ms_2}\right|\right)\right|$$
$$y_{ms_1} \neq \left| \left(\pm y_{ms_2} \pm j\left|x_{ms_1} - x_{ms_2}\right|\right)\right|$$

which conforms well with the matrix definition (53) for the evaluation of constants *a* and *b* as well.

A brief description is provided to explain the conditions. The first constraint forces the imaginary quantities to be non-zero so that a 2-D evaluation can be obtained, which is not possible if either or both of them are zero. This is hence a deviation from the conventional evaluation in the real domain. Further, the next two constraints force the ratio $\left(\left|\frac{x_{ms_1} - x_{ms_2}}{y_{ms_1} \pm y_{ms_2}}\right|\right)$ and its inverse to exist and not equal unity. This constraint has to be satisfied as the magnitude of the response of the two specimens has to be different for a particular input and hence the constraint prohibits the selection of specimens which do not obey the ratio constraint. Also, since the ratio is not unity, the scaling in the specimen domain is non-linear when two sets of specimens are used, which is essential, as described earlier. Note also that all of the analysis procedures generated square matrices which can be inverted. The working procedure of the process is illustrated with a numerical example.

3.2 APPLICATIONS - A NUMERICAL EXAMPLE

The quadratic and cubic processes are illustrated with the help of a numerical example where the stress of an aluminum product plate of circular geometry and 2 *in* radius is predicted based on two square aluminum product specimen plates of 16 in^2 and 4in^2 area respectively. A nylon model plate of circular geometry and 1 *in* radius, and two square nylon model specimen plates of 4 in^2 and 1in^2 area respectively are

the other geometries used. Note that the ratio of the areas in the specimen domain is maintained at 4 in both cases as required by geometric similarity. Further, this example is the most appropriate to the study as the geometries chosen are exactly in conformance with the initial mapping shapes. All geometries are of negligible thickness (so that a close 2-D approximation is valid), and a non-linear compressive load is applied on one face of any geometry while the other face is fixed (no rotation or translation) such that the response of the system is elongation only in the directions perpendicular to the load. The compressive stresses formed are distributed along the surface where each and every point on the surface is subjected to elongation, the maximum elongation occurring at the very edges of the geometry. Hence if a point *R* on the surface is defined by a complex number,

$$z = u + iv \tag{54}$$

then the elongation produced and the strain developed are respectively given by,

$$\partial z = \partial u + i\partial v$$
$$\varepsilon = \frac{\partial z}{|z|} = \frac{\partial u + i\partial v}{\sqrt{u^2 + v^2}} = \frac{\partial z}{\sqrt{z\bar{z}}} \tag{55}$$

assuming that the derivative exits the function is analytic and satisfies the Cauchy – Reimann conditions. This strain is direction and property dependent and hence, for an anisotropic material, the extent of elongation depends on the variation of material properties along that direction. If the loading direction is along the *z* - axis out of (or into) the plane of the solid plate, then the elongation is purely in the *x*- and *y* – directions (see Figure 3). Hence, the stresses produced are due to the stretching of each point in the plane by an extent unique to the properties along the stretch direction. For simplicity in analysis, assuming an isotropic material, the stresses formed reach a numerical magnitude given by,

$$\sigma = E\frac{\partial z}{\sqrt{z\bar{z}}} \tag{56}$$

Re-arranging the terms by converting to radial distance and angles, we have,

$$\sigma = \left[E\left(\frac{\partial r + ir\partial\theta}{r} \right) e^{i\theta} \right] \tag{57}$$

and hence for the product,

$$\sigma_p = \left[E_p \left(\frac{\partial r_p + ir_p \partial\theta_p}{r_p} \right) \exp\left(i\theta_p\right) \right]$$

Simplifying further, consider a point infinitesimally close to the imaginary axis for ease in analysis. Then,

$$\left|\sigma_p\right| \approx \left| E_p \left(\frac{i\partial y_p}{y_p} \right) \right| = \left| E_p \left(i\varepsilon_p \right) \right| \tag{58}$$

Further, differentiating the model equations for both second and third order polynomials assuming that a point close to the imaginary axis is being evaluated and letting all real parts of the equations to be null, the second and third order estimates converge as all the factors tend to be null except for the constants that are co-efficients of the z^1 term *i.e.*, *B* and *C* in the second and third order polynomial respectively. Therefore,

$$\frac{\partial y_p}{y_p} = \frac{e^{aC} \exp\left\{ \frac{A}{a} \left\{ \ln\left(iv_m\right) \right\}^2 \right\} \left\{ \left(iv_m\right) \right\}^{B-1} \left[B + \frac{2A}{a} \left\{ \ln\left(iv_m\right) \right\} \right] \partial v_m}{\left| \left\{ \left(iv_m\right) \right\}^B e^{aC} \exp\left\{ \frac{A}{a} \left\{ \ln\left(iv_m\right) \right\}^2 \right\} \right|}$$

or

$$\left| \frac{i\partial y_p}{y_p} \right|_2 = \frac{\partial v_m \left[B + \frac{2A}{a} \left| \left\{ \ln\left(iv_m\right) \right\} \right| \right]}{v_m} \tag{59}$$

Using the Taylor Series Expansion for the logarithmic function and neglecting higher order terms,

$$\left| \frac{i\partial y_p}{y_p} \right|_2 = \frac{\partial v_m \left[B + \frac{4A}{a} \left| \left(\frac{iv_m - 1}{iv_m + 1} \right) \right| \right]}{v_m} = \frac{\partial v_m \left[B + \frac{4A}{a} \left| \left(\frac{1 - 2iv_m - v_m^2}{v_m^2 + 1} \right) \right| \right]}{v_m}$$

or

$$\left| \frac{i\partial y_p}{y_p} \right|_2 \le \frac{\partial v_m \left[B + \frac{4A}{a\left(v_m^2 + 1\right)} \left\{ \sqrt{4v_m^2 + \left(1 - v_m^2\right)^2} \right\} \right]}{v_m} \tag{60}$$

since $\left|z_1 + z_2 + z_3\right| \le \left|z_1\right| + \left|z_2\right| + \left|z_3\right|$

and

$$\left| \frac{i\partial y_p}{y_p} \right|_2 = \left|i\varepsilon_p\right| \le \left| \frac{\partial v_m \left[B + \frac{4A}{a} \right]}{v_m} \right| = \left(B + \frac{4A}{a} \right) \varepsilon_m$$

Hence,

$$\sigma_p \approx \left[E_p \left(B + \frac{4A}{a} \right) \varepsilon_m \right] \tag{61}$$

Similarly,

$$\left| \frac{i\partial y_p}{y_p} \right|_3 = \left| i\varepsilon_p \right| \le \left| \frac{\partial v_m \left[C + \frac{4B}{a} + \frac{6A}{a^2} \right]}{v_m} \right| = \left(C + \frac{4B}{a} + \frac{6A}{a^2} \right) \varepsilon_m$$

and hence,

$$\sigma_p \approx \left[E_p \left(C + \frac{4B}{a} + \frac{6A}{a^2} \right) \varepsilon_m \right] \tag{62}$$

Further,

$$a = \lim_{u_m \to 0} \frac{1}{y_{ms}} \tan^{-1} \left(\frac{v_m}{u_m} \right) = \lim_{\theta_m \to \frac{\pi}{2}} \frac{\theta_m}{y_{ms_1}} = \frac{\pi}{2y_{ms}} \tag{63}$$

and

$$b = \lim_{u_m \to 0} \frac{1}{y'_{ms}} \tan^{-1} \left(\frac{v_m}{u_m} \right) = \lim_{\theta_m \to \frac{\pi}{2}} \frac{\theta_m}{y'_{ms}} = \frac{\pi}{2y'_{ms}} \tag{64}$$

The comprehensive analysis performed for the stress parameter has highlighted two important results:

- Comparing Equations (61) and (62), the strength value is independent of the constant term in the polynomial variation. Further, if the constant is assumed to be of zero magnitude, then the polynomial curve, indicating strain, passes through the origin and so does the stress curve. From solid mechanics, this is the definition of the standard stress-strain curve. Hence the analysis is in direct correlation with theory.
- Equations (61) and (62) also indicate a pattern in the stress values that is summarized below.

For a conformal map between the basic shapes of circles and rectangles (*squares*), *if the response parameter of interest* (*stress*) *is estimated at a point close to the imaginary axis, assuming the material to be isotropic and uniform in properties, the stress is given by the formula*:

$$\sigma_p \approx \left[E_p \left\{ \sum_{k=1}^{n} \left(\frac{2kA_{k-1}}{a^{k-1}} \right) \right\} \varepsilon_m \right] \tag{65}$$

where $2A_0$ represents the co-efficient of the z^1 term for a polynomial definition given by:

$$f(z) = B_0 + B_1 z + B_2 z^2 + \ldots + B_n z^n \tag{66}$$

The factor a (b) thus compensates for the structural distortion and the constants in the polynomial transformation account for the non-linear variations in material properties. Contrasting equations (62) and (63), these constants define the scaling laws in the ESM procedure.

The geometries mentioned above were tested for different non-linear loading patterns and the deformation examined for the evaluation of elongation. A 3-D modeling and analysis package, SolidWorks®, was used for finite element analysis of the geometries to establish the change in the shape of the plates for different loading schemes and the values tabulated and compared.

From classical mechanics, it is well known that the maximum stress is experienced by the object at its very boundaries (edges) due to one face of its geometry being constrained in motion in both directions perpendicular to the loading direction, which is illustrated by the pictures plotted below (see Figure 3). The loading conditions are non-linear force values simulated using a random number generation function for a normal distribution with a mean of 100 and a standard deviation of 10.

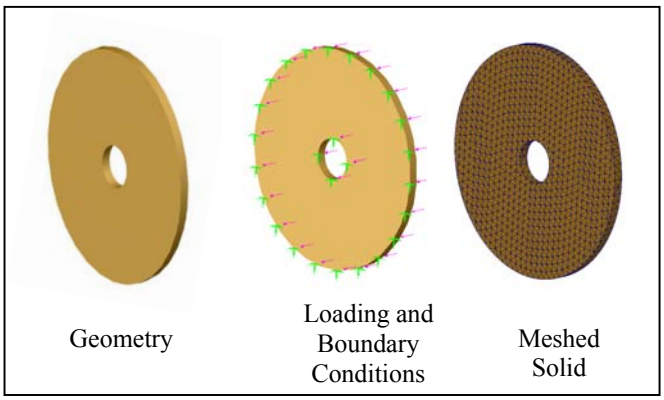

Figure 3. Product Geometry, Loads and Meshing

The stress plots and the predicted stress plot are shown in Figures 4 through 6 to illustrate the results of conformal mapping. Note that the stresses shown are at the perimeter of the surface for different loading conditions.

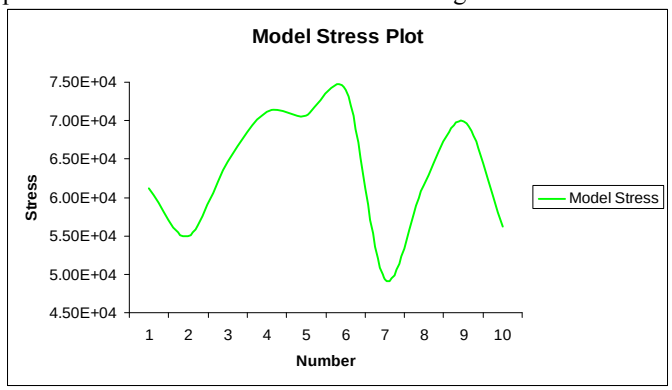

Figure 4. Model Stress Curve

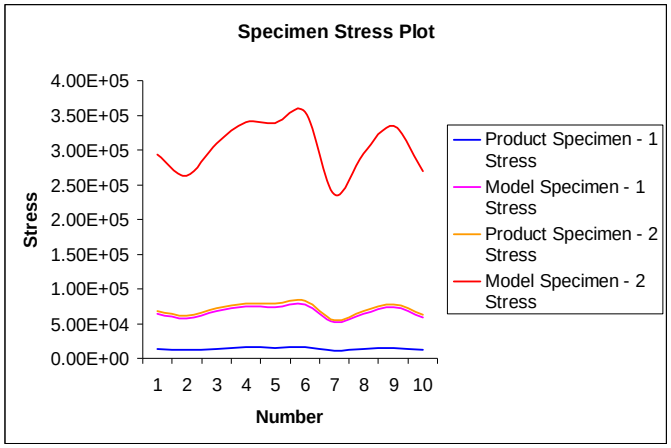

Figure 5. Model Specimen and Product Specimen Stress Curves

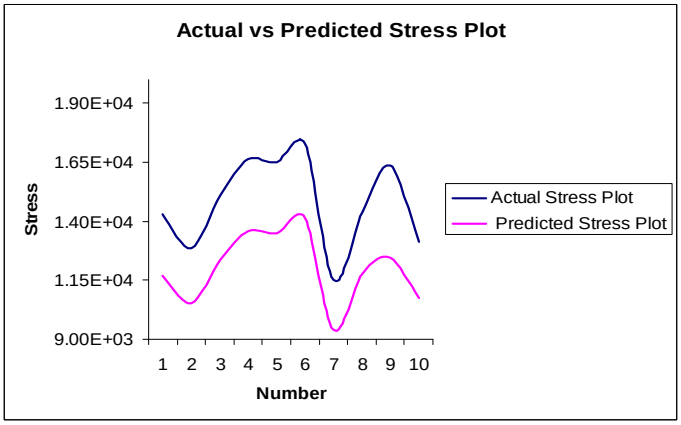

Figure 6. Product Stress Plots

As is observed in Figure 6 the mapping provided a similar trend in stress variation as is obtained from the FEM analysis. Importantly, the process did not require the specification of mesh types or sizes nor did there arise any necessity for using iterative solutions as the process is more deterministic. However, there is a discrepancy in the actual values obtained which is discussed in the next section.

3.3 ERROR ANALYSIS

The plots developed for the actual stress and the predicted stress follow the same pattern indicating a successful map in terms of angles and relative distances. However there is a discrepancy in the actual stress value obtained. The average predicted error obtained is about 18%. An initial error analysis is discussed here to identify the contributing factors for this error.

The models used in the FEM analysis have been assumed to be linear isotropic due to the limited options available in the analysis package. Nylon, being a polymer is anisotropic and thus has non-linear response patterns.

There is a second form of error that is intuitively apparent but not very obvious from the analysis. This error is generated due to the stress concentrations that occur in the square nylon plates at the tips and edges. This stress concentration can be visualized as a stress field developed at the very perimeter of the surface that is unaccounted for and incorrectly mapped by the transformations of the points on the circumference of the surface. A more detailed analysis for point locations on perimeters is discussed in this regard to initiate a more rigorous approach to stress concentration modeling. Recall that a point on the perimeter defined by a complex coordinate 'z' was hypothesized to be elongated by a distance ∂z which is the change in distance from its equilibrium position. The stress concentration occurring at the edges can be mathematically thought of as a collection of points that are elongating differently and at different rates from most other points on the surface. The integral used for evaluating the stress used an ideal '∂z' which assumed that all points elongated at the same rate.

A third form of error is the truncation error from the Taylor Series Expansion. Recall, that the expansion was truncated at the first order terms and hence the estimate obtained is of first order accuracy and has an inherent truncation error.

Hence the factors that contribute towards the error and their individual contributions are just as important as the value of the net error. Since it is a fair assumption, that stress concentrations are the most common form of distortion of stress values, most systems are often associated with a factor of safety that scales the calculated stress to a more realistic value. However, in the case of complex variables analysis, it is very complicated to single out a numerical value for the factor of safety. This is addressed by a process called the Iso-potential lines approach, which is discussed in the future work section of the paper.

Keeping in mind the necessity to provide a rational explanation for the amount of loss due to stress concentration, another approach is elucidated by treating the stress concentration as a distortion parameter. The following example examines the process for such distortions.

3.4 A HEAT TRANSFER PROBLEM

A heat transfer problem is now illustrated to highlight the applicability of ESM in situations involving distortion, similar to the example provided in [Dutson, 2002]. In this example the steady state temperature of the product is the variable of interest. The idea is to evaluate the steady state temperature of the product based on multiple readings at corresponding points in the model. Assume that the materials used are the same as in the previous example. Let the surface of the product and product specimens be subjected to a temperature of 600K (green contours) and the internal surfaces to a temperature of 300K (blue contours). For the purpose of analysis, let the hypothetical maximum temperature that the model and model specimens material can withstand be 450K (red contours), then ESM can be used for prediction since we

have simulated a distortion situation as for TSM, $\left(\frac{T_o}{T_i}\right)_p = \left(\frac{T_o}{T_i}\right)_m$ is required and actually $\left(\frac{600K}{300K}\right) \neq \left(\frac{450K}{300K}\right)$. Hence ESM is relevant and applicable. The simplified geometry of the specimen pairs, along with the overall ESM setup for the problem, is shown in Figure 7.

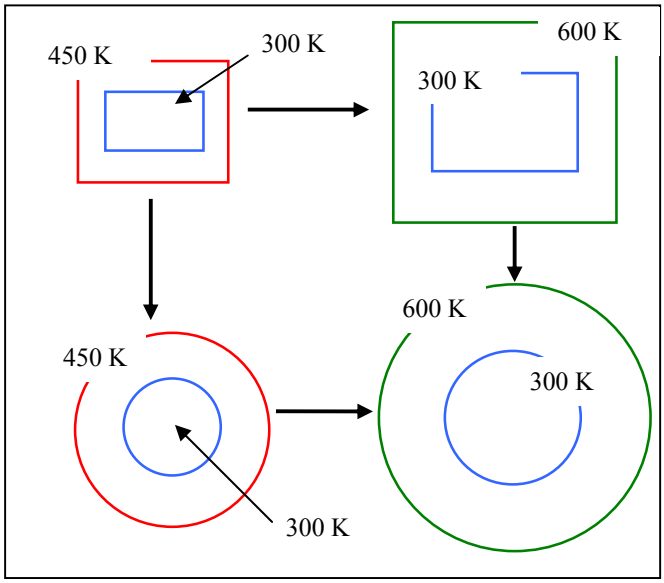

Figure 7. ESM Setup for Steady- State Temperature

The idea is to evaluate the steady state temperature of a multiple points in the annular region of the product along the imaginary (vertical) axis. These points are translated into the specimen domain where they can be located using a simple linear interpolation between the concentric rectangles.

Note that the model and model specimen material (Nylon) is thermally more resistant than the product system (made from Aluminum). The distortion that is now intended to be captured is from the effect of thermal expansion and hence thermal stress that the product system is subjected to. The change in geometry due to thermal variation is negligible in the model system while it is considerable in the product system thereby inducing a distortion between the two systems.

Since scaling temperatures is complicated an easier alternative is used. From fundamental heat transfer, length of a specimen changes with temperature according to the formula,

$$l = l_0(1 + \alpha\Delta T) \tag{66}$$

where l_0 is the equilibrium length, α is the coefficient of linear expansion and ΔT is the change in the temperature. Rewriting the equation in complex variables,

$$\frac{\partial z}{|z|} = \alpha\Delta T \tag{67}$$

and hence

$$\varepsilon_p = \alpha_p\left(T_p - T_0\right) \tag{68}$$

where T_0 is the lower boundary temperature and ε_p is the strain of the product. From the relations developed for the stress example, we know that the strain of the product can be associated with that of the model using the relationship,

$$\left|\varepsilon_p\right| \le \left|\frac{\partial v_m\left[B + \frac{4A}{a}\right]}{v_m}\right| = \left(B + \frac{4A}{a}\right)\varepsilon_m$$

Hence, we have,

$$T_p = T_0 + \left(B + \frac{4A}{a}\right)\left(\frac{\varepsilon_m}{\alpha_p}\right) \tag{69}$$

and more specifically for each point,

$$T_{p,i} = T_{O,i} + \left(B + \frac{4A}{a}\right)\left(\frac{\varepsilon_m}{\alpha_p}\right) \tag{70}$$

Before proceeding to a full-fledged FEM analysis, a brief examination of the equation suggests that the linear formulation is valid since the strain ε_m is of zero magnitude when the two temperatures are equal. Further the temperature T_p is maximum at the outer boundary when the elongation and hence the strain is the greatest.

The materials are once again tested for numerical accuracy using SolidWorks® analysis software. The product is a circular plate made of aluminum with geometric specifications of 4 *in* outer diameter and 2 *in* inner diameter for the concentric hole. The model is also a circular plate made from nylon with a 2 *in* outer diameter and 1 *in* inner diameter for the concentric hole. The model specimen is made from nylon and has a geometry of 1 in^2 area with an inner hole area of 0.25 in^2 while the product specimen is made from aluminum and has a geometry of 4 in^2 area with an inner hole area of 1 in^2. The results of analysis are presented below.

Figure 8 and 9 illustrate the temperature variation (measured in Kelvin) for the aluminum circular plate and the nylon square plate. A fringe – line view is shown to illustrate the flow of temperature lines from the outer higher temperature to the inner lower temperature. The process of conformal mapping is to be done such that a similar map can be reproduced based on the responses from the model and the specimen pair. Further, in this case one specimen pair would suffice for the calculations as multiple readings are taken which would be sufficient to evaluate the constants. A more

detailed discussion is provided in the requirements and constraints section of the paper.

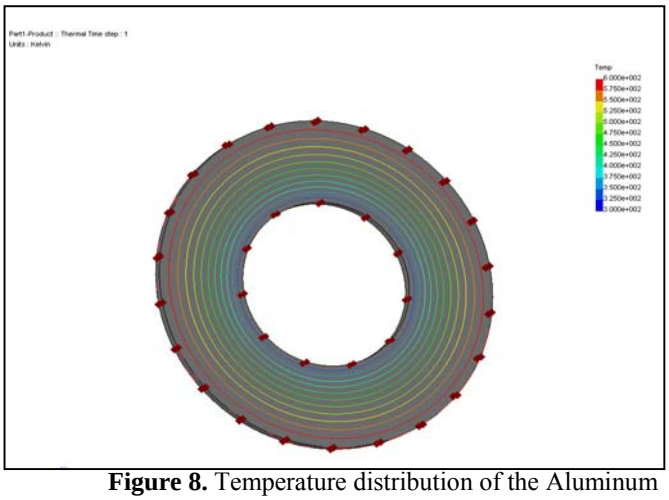

Figure 8. Temperature distribution of the Aluminum Product plate

Assume the points under evaluation (10) are equidistant from the inner perimeter to the outer circumference. Then each point (including the end-points) is at a distance of,

$$z_{po\,\mathrm{int}} = z_i + \left(\frac{z_o - z_i}{9}\right)$$

where z_0 and z_i are the distances in the *y*-axis of the inner and the outer peripheries respectively.

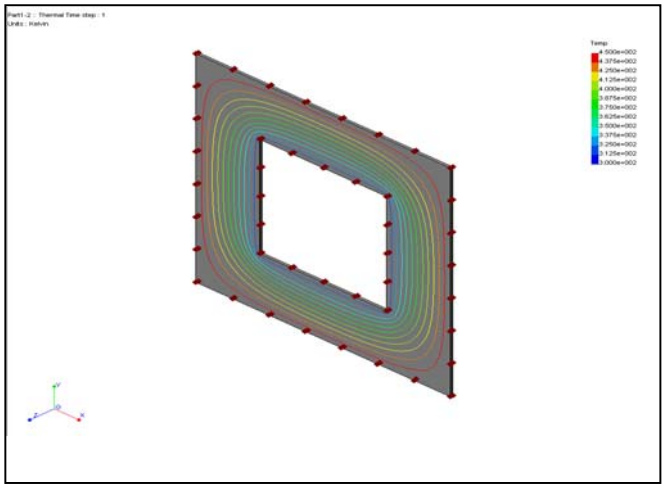

Figure 9. Temperature distribution of the Nylon Model Specimen plate

The temperature plots and the prediction plots are illustrated here.

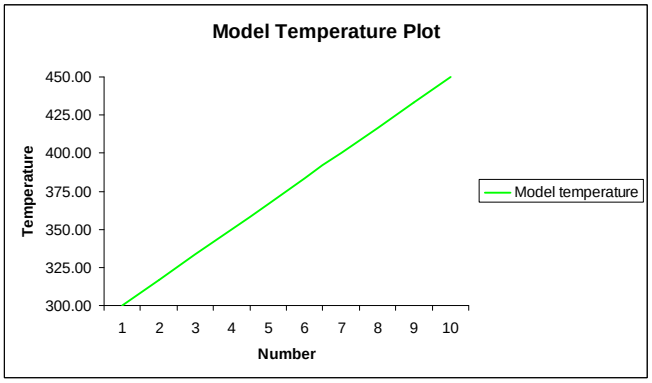

Figure 10. Model Temperature Plot

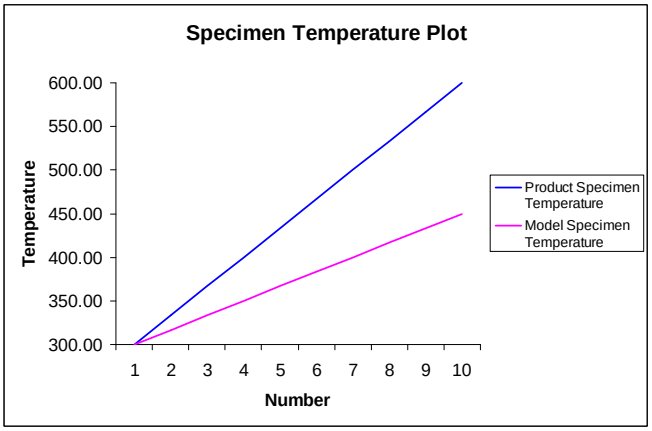

Figure 11. Specimen Temperature Plot

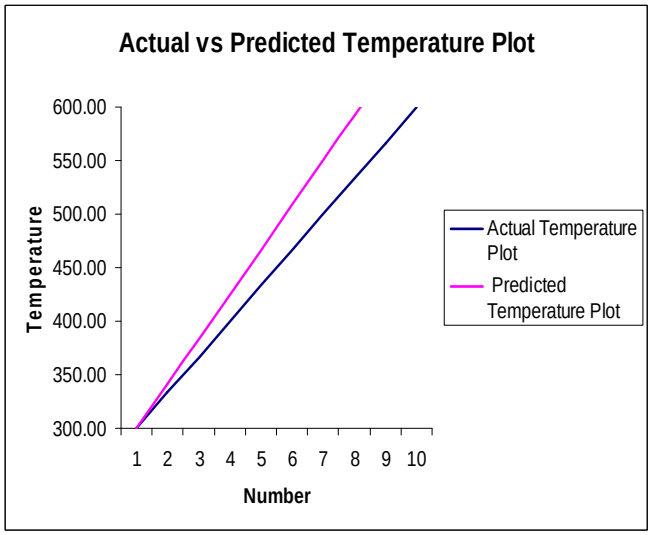

Figure 12. Product Temperature Plots

As is observed from the curves illustrated, the system response is fairly linear and the average error of about 7.5% is obtained (toward the higher side) signifying that an accurate mapping was obtained. However, another interesting pattern observed is that error increases with increase in temperature variation and hence capturing distortion needs smaller and more precise measurement distances.

3.5 CONFORMAL MAPPING – REQUIREMENTS AND CONSTRAINTS

The polynomial definition generated for the form transformation introduced the need for another set of intermediate specimens. A note is given here to emphasize that this is not the only solution for an exact evaluation. In order to determine the coefficients, two other approaches can be used.

The first alternate solution is to derive enough data points from the testing of a single specimen set to obtain an exact solution while the second solution is to fit a least squares curve for a selected few data points. The approach of using another specimen set is chosen since it is reasonable and economically feasible for lower order polynomial estimations. However, for complex evaluations involving higher order calculations, using more specimen sets is not a viable alternative due to time and cost constraints and hence one of the other two methods needs to be employed.

The technique of conformal mapping has been elucidated with the working procedure and the conditions for prediction. A word of caution is provided here to highlight the importance of maintaining mathematical integrity while using this process. The logarithmic function is multi-valued and hence has to be coerced to a single value using a branch cut. Further, the analysis presented assumes that the logarithmic function is defined in the complex plane such that it is single valued. A multi-valued function assumes different values depending on the angular orientation of the function. The logarithmic function defined by,

$$\ln z = \ln\left(re^{i\theta}\right)$$

is multi-valued as,

$$\begin{aligned}\ln\left(re^{i\theta}\right) &= \ln\left[r\exp\left\{i\left(\theta+2k\pi\right)\right\}\right] \\ &= \ln r + \left\{i\left(\theta+2k\pi\right)\right\}\end{aligned}$$

The value of the function changes depending on the value of the factor *k*, which denotes the number of counter clockwise rotations of the function about origin. Hence for every rotation, a distinct value of the function is obtained thereby necessitating using a branch cut to restrict the function to a single value by imposing a boundary curve that the function is constrained from crossing. Note that in the analysis procedure and in the two examples, points considered for evaluation were peripheral co-ordinates of the 2-D object *i.e.*, points on the circumference of the surface. This is required as the mapping is valid only for these points.

Understandably, the process of conformal mapping as an ESM procedure is still in its nascent stage but has shown considerable promise. While established analysis techniques such as FEM are more widely accepted, conformal mapping for scaling and similitude has been more dormant as an evaluation procedure. The motivation thus lies in proving its viability along similar lines as Joukowski's transformation that has facilitated understanding of the airfoil behavior based on the conformal mapping of the fluid flow across a cylinder [Grewal, 1998].

The transformations used in conformal mapping thus track geometry and loading conditions along with the boundary conditions and map all of them to simpler systems for easy evaluation. But not all systems can be mapped easily and require discretized simplifications. In this sense, conformal mapping is similar to FEM. However it has advantages over FEM techniques as the boundary conditions need not be separately specified and there is no necessity to specify mesh sizes, mesh types, sensitivity and accuracy required, processing time, computing capability etc. Conversely choosing a system transformation for a conformal map is an extremely difficult process for intricate mechanical systems and requires numerous approximations and adjustments. But as research seeks to obtain a systematic methodology for selecting such a system transformation, conformal mapping may prove to be an ideal analysis procedure.

4.0 CONCLUSIONS AND FUTURE WORK

The shape of the product is governed by numerous factors that include functionality, ergonomics and human factors, reliability, thermal and dynamic stability, control and operation feasibility, flexibility and failure modes, ease of manufacturability etc among others. This therefore limits the designer's freedom in choosing the final shape or geometry of the product. But if the technique of conformal mapping were to be used to quantify each of the factors listed above and their impact on the shape of the product, then the designer would benefit in terms of financial and functional independence. This would also significantly reduce testing and possible re-configuration time and hence the production time and cost.

The technique of conformal mapping has been known for a long time but its possible use as a scientific tool for similitude is novel and needs further exploration. A significant amount of work has also been done in the field of vector calculus and complex algebra and analysis to construct Green Functions using conformal mapping. This technique is of importance as it numerically defines the area of influence or the boundaries of application validity.

The study thus far has shown encouraging results and has identified several areas of interest which require further investigation.

The process is now being studied for rigid materials to account for the effect of anisotropy in comparison with the polymer models. A novel approach of determining safety factors is being pursued, using the concept of iso-potential lines such that discrete material forms with non-linear variations can be included in the technique. Repetitive mapping of surfaces is required for infinite open maps and an algorithm for such a mapping is being developed.

The procedure itself can be bettered if the technique is extended to irregular structures – symmetric and un-symmetric. This would form the basis for mappable geometries and hence will be a heuristic for the determination of form factors. These factors are hypothesized to be indicative of geometries that can be actually transformed and

mapped for analysis. The motivation lies in the development of an innovative prediction procedure with a well-developed methodology for selecting transformations and, well-defined governing set of laws.

REFERENCES

Bridgman, P. W. 1931. Dimensional Analysis, Yale University Press, New Haven.

Cho, U., and Wood, K., 1997, "Empirical Similitude Method for the Functional Test with Rapid Prototypes," *Proceedings of the Solid Freeform Fabrication Symposium*, Austin TX, September, 1997, pp. 559-567.

Cho, U., Wood, K. L., and Crawford, R. H., 1998, "Online Functional Testing with Rapid Prototypes: a Novel Empirical Similarity Method," *Rapid Prototyping Journal*, 4, No. 3, pp. 128-138.

Cho, U., Wood, K. L., and Crawford, R. H., 1998b, "Novel empirical similarity method for the reliable product test with rapid prototypes," *Proceedings of DETC*, Atlanta, GA, Sept. 13-16, 1998.

Cho, U., 1999, Novel Empirical Similarity Method for Rapid Product Testing and Development, Doctoral dissertation, The University of Texas at Austin.

Dutson, A.J, 2002, *Functional Prototyping Through Advanced Similitude Techniques*, Doctoral dissertation, The University of Texas at Austin.

Grewal, B.S., 1998, *Higher Engineering Mathematics*, Khanna Publishers, Delhi

Szirtes, T., 1998, Applied Dimensional Analysis and Modeling, McGraw-Hill, New York.

Schinzinger, R., Laura, P. A. A., 1991, *Conformal Mapping: Methods and Applications*, Elsevier Science Publishers B.V.

Wood, J. J., and Wood, K. L. 2002b. "Empirical Analysis using Advanced Similarity Methods," *Proceedings of DETC* 2002.